ResearchGate

See discussions, stats, and author profiles for this publication at: https://www.researchgate.net/publication/11281222

Comparison of the binding of cadmium(II), mercury(II), and arsenic(III) to the de novo designed peptides TRI L12C and TRI L16C

ARTICLE *in* JOURNAL OF THE AMERICAN CHEMICAL SOCIETY · AUGUST 2002

Impact Factor: 12.11 · DOI: 10.1021/ja017520u · Source: PubMed

CITATIONS
93

READS
50

6 AUTHORS, INCLUDING:

Manolis Matzapetakis
New University of Lisbon
31 PUBLICATIONS **939** CITATIONS
SEE PROFILE

James Penner-Hahn
University of Michigan
272 PUBLICATIONS **10,035** CITATIONS
SEE PROFILE

Vincent L Pecoraro
University of Michigan
313 PUBLICATIONS **12,799** CITATIONS
SEE PROFILE

Available from: Vincent L Pecoraro
Retrieved on: 24 January 2016

J|A|C|S
ARTICLES
Published on Web 06/17/2002

Comparison of the Binding of Cadmium(II), Mercury(II), and Arsenic(III) to the de Novo Designed Peptides TRI L12C and TRI L16C

Manolis Matzapetakis,[†] Brian T. Farrer,[†] Tsu-Chien Weng,[†] Lars Hemmingsen,[‡] James E. Penner-Hahn,[†] and Vincent L. Pecoraro*[,†]

Contribution from the Department of Chemistry, University of Michigan, Ann Arbor, Michigan 48109-1055, and the Department of Mathematics and Physics, Royal Veterinary and Agricultural University, Thorvaldsensvej 40, DK-1871, Frederiksberg C, Denmark

Received November 12, 2001

Abstract: Designed α-helical peptides of the TRI family with a general sequence Ac-G(LKALEEK)$_4$G-$CONH_2$ were used as model systems for the study of metal−protein interactions. Variants containing cysteine residues in positions 12 (TRI L12C) and 16 (TRI L16C) were used for the metal binding studies. Cd(II) binding was investigated, and the results were compared with previous and current work on Hg(II) and As(III) binding. The metal peptide assemblies were studied with the use of UV, CD, EXAFS, ^{113}Cd NMR, and ^{111m}Cd perturbed angular correlation spectroscopy. The metalated peptide aggregates exhibited pH-dependent behavior. At high pH values, Cd(II) was bound to the three sulfurs of the three-stranded α-helical coiled coils. A mixture of two species was observed, including Cd(II) in a trigonal planar geometry. The complexes have UV bands at 231 nm (20 600 M^{-1} cm^{-1}) for TRI L12C and 232 nm (22 600 M^{-1} cm^{-1}) for TRI L16C, an average Cd−S bond length of 2.49 Å for both cases, and a ^{113}Cd NMR chemical shift at 619 ppm ($Cd^{II}(TRI\ L12C)_3^-$) or 625 ppm ($Cd^{II}(TRI\text{-}L16C)_3^-$). Nuclear quadrupole interactions show that two different Cd species are present for both peptides. One species with $\omega_0 = 0.45$ rad/ns and low η is attributed to a trigonal planar Cd−$(Cys)_3$ site. The other, with a smaller ω_0, is attributed to a four-coordinate Cd-$(Cys)_3(H_2O)$ species. At low pH, no metal binding was observed. Hg(II) binding to TRI L12C was also found to be pH dependent, and a 3:1 sulfur-to-mercury(II) species was observed at pH 9.4. These metal peptide complexes provide insight into heavy metal binding and metalloregulatory proteins such as MerR or CadC.

Over the past decade, de novo peptide design has emerged as an important approach for understanding protein folding, structure. and function.[1−5] While many structural motifs such as α/β proteins,[6−10] β-sheet proteins,[6,11,12] and collagens[6,7] have been targeted, the vast majority of the work has focused on the preparation of α-helical bundles and coiled coils.[1,6,13−15] The simplicity of the coiled coil structure, which uses right-handed, amphipathic α-helices as the primary secondary structural element, has allowed numerous investigators to address issues of protein folding. Among these issues are the orientation of the helices (parallel vs antiparallel),[16−19] aggregation of the peptides (two-, three-, or four-stranded coiled coils),[20,21] and the overall stability of bundle formation, which can be affected by chain length and amino acid composition.[21,22] More recently, the interaction of coiled coils with metals has also been

* To whom correspondence should be addressed. Phone: 734-763-1519. Fax: 734-936-7628. E-mail: vlpec@umich.edu.
[†] University of Michigan.
[‡] Royal Veterinary and Agricultural University.

(1) DeGrado, W. *Science* **1997**, *278*, 80−81.
(2) Gibney, B.; Rabanal, F.; Dutton, P. *Curr. Opin. Chem. Biol.* **1997**, *1*, 537−542.
(3) Bryson, J. W.; Betz, S. F.; Lu, H. S.; Suich, D. J.; Zhou, H. X. X.; Oneil, K. T.; Degrado, W. F. *Science* **1995**, *270*, 935−941.
(4) Kohn, W. D.; Hodges, R. S. *Trends Biotechnol.* **1998**, *16*, 379−389.
(5) Benson, D. E.; Wisz, M. S.; Hellinga, H. W. *Proc. Natl. Acad. Sci. U.S.A.* **2000**, *97*, 6292−6297.
(6) DeGrado, W.; Summa, C.; Pavone, V.; Nastri, F.; Lombardi, A. *Annu. Rev. Biochem.* **1999**, *68*, 779−819.
(7) Hodges, R. S.; Saund, A. K.; Chong, P. C. S.; Stpierre, S. A.; Reid, R. E. *J. Biol. Chem.* **1981**, *256*, 1214−1224.
(8) Houbrechts, A.; Moreau, B.; Abagyan, R.; Mainfroid, V.; Preaux, G.; Lamproye, A.; Poncin, A.; Goormaghtigh, E.; Ruysschaert, J. M.; Martial, J. A.; Goraj, K. *Protein Eng.* **1995**, *8*, 249−259.
(9) Pujadas, G.; Palau, J. *Biologia* **1999**, *54*, 231−253.
(10) Silverman, J. A.; Balakrishnan, R.; Harbury, P. B. *Proc. Natl. Acad. Sci. U.S.A.* **2001**, *98*, 3092−3097.
(11) Cox, A.; Arroyo, M. M.; Mayo, K. H. *Biochem. J.* **2001**, *357*, 739−747.
(12) Xu, G. F.; Wang, W. X.; Groves, J. T.; Hecht, M. H. *Proc. Natl. Acad. Sci. U.S.A.* **2001**, *98*, 3652−3657.
(13) Hodges, R. S. *Biochem. Cell Biol.* **1996**, *74*, 133−154.
(14) Dieckmann, G.; McRorie, D.; Tierney, D.; Utschig, L.; Singer, C.; OHalloran, T.; PennerHahn, J.; DeGrado, W.; Pecoraro, V. *J. Am. Chem. Soc.* **1997**, *119*, 6195−6196.
(15) Lupas, A. *Trends Biochem. Sci.* **1996**, *21*, 375−382.
(16) Monera, O. D.; Zhou, N. E.; Lavigne, P.; Kay, C. M.; Hodges, R. S. *J. Biol. Chem.* **1996**, *271*, 3995−4001.
(17) Oakley, M. G.; Hollenbeck, J. J. *Curr. Opin. Struct. Biol.* **2001**, *11*, 450−457.
(18) Suzuki, K.; Hiroaki, H.; Kohda, D.; Nakamura, H.; Tanaka, T. *J. Am. Chem. Soc.* **1998**, *120*, 13008−13015.
(19) Morii, H.; Ishimura, M.; Honda, S.; Uedaira, H. *Protein Eng.* **1995**, *8*, 56−56.
(20) Tripet, B.; Wagschal, K.; Lavigne, P.; Mant, C. T.; Hodges, R. S. *J. Mol. Biol.* **2000**, *300*, 377−402.
(21) Wagschal, K.; Tripet, B.; Hodges, R. S. *J. Mol. Biol.* **1999**, *285*, 785−803.
(22) Su, J. Y.; Hodges, R. S.; Kay, C. M. *Biochemistry* **1994**, *33*, 15501−15510.

10.1021/ja017520u CCC: $22.00 **© 2002 American Chemical Society**

Scheme 1. Sequence of TRI Peptides

TRI	Ac-G LKALEEK LKALEEK LKALEEK LKALEEK G-$CONH_2$
TRI L12C	Ac-G LKALEEK LKA<u>C</u>EEK LKALEEK LKALEEK G-$CONH_2$
TRI L16C	Ac-G LKALEEK LKALEEK <u>C</u>KALEEK LKALEEK G-$CONH_2$

investigated because of the importance of metals as protein structural determinants and catalytic centers in natural proteins.[6,23−27] Coordination of a metal to a peptide may be accompanied by a change in the peptide structure,[14,18,27,28] the generation of exogenous ligand binding sites,[29,30] or the introduction of a site for electron transfer or catalysis. Thus, a number of effects determine the overall structure of metallopeptides.

Several strategies for designing metalloproteins have been advanced. In one protein engineering approach, investigators modified the existing scaffolding of a biomolecule to incorporate a metal ion into the natural fold of a protein that has a different function.[31] In this way, one may exploit the inherent stability of the native protein fold to introduce a metal into a desired coordination environment. Alternatively, several examples of α-helices containing modified heptad repeats are known that will self-aggregate to generate metal binding sites.[14,18,32] Also, tethered amphipathic α-helices form four-stranded bundles that have been demonstrated to bind hemes,[33] metalloporphyrins,[34] binuclear metal centers, and Fe_xS_x clusters.[35] Combinatorial algorithms have been used to prepare very stable Zn finger motifs.[36] In early designed metalloproteins, the incorporated metal is on the surface of the assembly or bound to peripheral, unnatural amino acids containing ligands such as bipyridyl groups.[29,30] In most cases studied to date, sites for hard Lewis acids have been generated; however, metal binding sites for softer metals such as Hg(II), As(III), Cd(II), and Pb(II) have appeared recently.[14,27,37]

We have been interested in several issues pertaining to metalloprotein design. In our studies, we have used the amphipathic peptide TRI, which consists of four repetitions of the heptad Leu_a-Lys_b-Ala_c-Leu_d-Glu_e-Glu_f-Lys_g, and single substituted variants with cysteine replacing leucine in the *a* or *d* positions (e.g., TRI L12C), as shown in Scheme 1.[14,38] First,-we have shown that designed peptides can exhibit pH-dependent aggregation state preferences (two-stranded bundles when pH < 5 and three-stranded bundles when pH > 7). This aggregation preference can be exploited to enforce uncommon coordination geometries on a metal. Second, we have illustrated that there is a subtle energetic balance between obtaining the less favorable peptide aggregation state that contains the preferred metal coordination geometry, or the more favored peptide bundle that contains a metal ion in an unusual coordination mode. Third, we have shown that the position of the cysteine substitutions can affect the coordination geometry of some metals (e.g., Hg(II)) but not others (e.g., As(III)). Fourth, we have been interested in defining the chemistry of heavy metals with proteins in order to establish how these metals may be responsible for toxicity in bacteria and mammals.

In this article, we present the synthesis and characterization of the TRI peptide series with Cd(II) bound in a novel three-coordinate trigonal geometry. Such low coordination numbers are rarely seen for Cd(II) in aqueous solution.[37] These results will be contrasted with the previously reported complexes of Hg(II) and As(III) under a variety of conditions. We also will reevaluate the relationship between the coordination number of bound mercury and the substitution pattern of the peptide (i.e., *a* vs *d* substitution).

Experimental Section

Peptide Synthesis and Purification. Peptides were synthesized on a Milligen 9050 automated peptide synthesizer using amino acids with −OPfp (pentafluorophenol) activating and Fmoc protecting groups (Novabiochem) and employing previously described procedures.[39] A Rink amide resin (Novabiochem) was used as a solid support, resulting in amidation of the C-terminus of the peptide product. The N-terminus was acetylated on the column using a solution of 4% acetic anhydride, 4.3% pyridine, and 91.7% DMF. Cleavage from the resin was performed for 90 min in a 90% trifluoroethanol (TFA) solution containing 5% anisol, 3% thioanisol, and 2% ethanedithiol as scavengers to protect the cysteine thiol moiety. After precipitation with cold ether, the peptide was redissolved in water and lyophilized to obtain a fluffy off-white powder. The solid was redissolved in 10% acetic acid and purified by reversed-phase HPLC using a preparative C18 column (Vydac Protein & Peptide) with a water/acetonitrile gradient. The gradient consisted of 0−100% solvent B over 50 min, where solvent A was 0.1% TFA in water and solvent B was 0.1% TFA in 9:1 CH_3CN:H_2O. The identity of the peptide was verified by matrix-assisted laser desorption/ionization time-of-flight (MALDI-TOF) and electrospray (ES) mass spectrometry, and the purity was determined by analytical HPLC to be >90%.

Fresh solutions of the purified peptide were prepared for each experiment using doubly distilled water containing the appropriate buffer. The peptide concentrations of these solutions were determined by quantitation of the cysteine thiols using Ellman's test,[40] which uses dithionitrobenzoate (DTNB) as an indicator. The concentrations of the metals in the metal standard solutions were determined by ICP atomic absorption spectroscopy. Metal solutions for experiments were prepared by serial dilutions of metal standards (1000 ppm cadmium in 2% HCl ICP standard (SPEX CertiPrep)) with buffer solutions.

Ultraviolet (UV) Titrations. Titrations to monitor the binding of metals to the peptides were performed on a Perkin-Elmer Lambda 9 UV−vis−NIR spectrophotometer. All spectra were collected from 210 to 310 nm, with a scan rate of 240 nm/s and a slit width of 4 mm, using a 1 cm quartz cell. Difference titration experiments were performed by subtracting the signal of a cuvette containing only buffer solution from the signal of a similar solution containing 10 μM $CdCl_2$ after adding equivalent aliquots of the peptide solution to both cuvettes. The extinction coefficients of the complexes were calculated from the

(23) Kennedy, M. L.; Gibney, B. R. *Curr. Opin. Struct. Biol.* **2001**, *11*, 485−490.
(24) Baltzer, L.; Nilsson, J. *Curr. Opin. Biotechnol.* **2001**, *12*, 355−360.
(25) Xing, G.; DeRose, V. J. *Curr. Opin. Chem. Biol.* **2001**, *5*, 196−200.
(26) Gibney, B. R.; Dutton, P. L. *Adv. Inorg. Chem.* **2001**, *51*, 409−455.
(27) Farrer, B. T.; McClure, C. P.; Penner-Hahn, J. E.; Pecoraro, V. L. *Inorg. Chem.* **2000**, *39*, 5422−5423.
(28) Ghadiri, M. R.; Case, M. A. *Angew. Chem., Int. Ed. Engl.* **1993**, *32*, 1594−1597.
(29) Lieberman, M.; Tabet, M.; Sasaki, T. *J. Am. Chem. Soc.* **1994**, *116*, 5035−5044.
(30) Mutz, M. W.; McLendon, G. L.; Wishart, J. F.; Gaillard, E. R.; Corin, A. F. *Proc. Natl. Acad. Sci. U.S.A.* **1996**, *93*, 9521−9526.
(31) Hellinga, H. W. *Fold. Des.* **1998**, *3*, R1−R8.
(32) Hill, R. B.; Raleigh, D. P.; Lombardi, A.; Degrado, N. F. *Acc. Chem. Res.* **2000**, *33*, 745−754.
(33) Gibney, B. R.; Huang, S. S.; Skalicky, J. J.; Fuentes, E. J.; Wand, A. J.; Dutton, P. L. *Biochemistry* **2001**, *40*, 10550−10561.
(34) Huffman, D. L.; Suslick, K. S. *Inorg. Chem.* **2000**, *39*, 5418−5419.
(35) Gibney, B. R.; Mulholland, S. E.; Rabanal, F.; Dutton, P. L. *Proc. Natl. Acad. Sci. U.S.A.* **1996**, *93*, 15041−15046.
(36) Dahiyat, B. I.; Mayo, S. L. *Science* **1997**, *278*, 82−87.
(37) Li, X. Q.; Suzuki, K.; Kanaori, K.; Tajima, K.; Kashiwada, A.; Hiroaki, H.; Kohda, D.; Tanaka, T. *Protein Sci.* **2000**, *9*, 1327−1333.
(38) Dieckmann, G.; McRorie, D.; Lear, J.; Sharp, K.; DeGrado, W.; Pecoraro, V. *J. Mol. Biol.* **1998**, *280*, 897−912.
(39) Choma, C. T.; Lear, J. D.; Nelson, M. J.; Dutton, P. L.; Robertson, D. E.; Degrado, W. F. *J. Am. Chem. Soc.* **1994**, *116*, 856−865.
(40) Ellman, G. L. *Arch. Biochem. Biophys.* **1959**, *82*, 70−77.

initial slopes of the titration curves and were based on the total metal concentration.

pH titrations were completed by the addition of small aliquots of potassium hydroxide to unbuffered solutions of 10 μM $CdCl_2$ and 40 μM peptide. The pH was monitored using a gel-filled combination electrode (Accumet) attached to a Fisher Accumet model 805 pH meter. To ensure reversibility of the transition, reverse titrations were performed subsequently by adding small amounts of HCl to the solution. To avoid the extraction of cadmium by chloride, the amount of chloride in the solution never exceeded 100 mM. Also, the solutions were constantly purged with argon, preventing significant buildup of disulfide-linked peptide dimers.

Circular Dichroism Spectroscopy. All CD spectroscopy was performed on an AVIV 62DS spectrometer using 1 cm strain-free quartz cuvettes. The peptide concentration for each experiment was 35 μM, with a metal concentration of 10 μM. The solutions were adjusted to pH 8.5 or 9.4 using small aliquots of a 1 M KOH solution with monitoring by using a gel-filled combination electrode (Accumet), while a 100 μM CHES buffer was used. All solutions were degassed with argon before the addition of the peptide and were prepared shortly before each measurement. Spectra were collected at 22 °C from 210 to 310 nm, averaging for 5 s at each point. The molar ellipticity, [Θ], is given in units of deg cm^2 dmol^{-1} and was calculated using eq 1, where θ_{obs} is the ellipticity in millidegrees, l is the path length of

$$[\Theta] = \theta_{obs}/(10lC) \quad (1)$$

the cell in centimeters, and C is the peptide concentration in moles per liter. The difference CD spectra are reported with molar ellipticities referenced to the total metal concentration.

Guanidinium denaturations were monitored at 222 nm and performed by mixing two stock solutions to afford guanidinium concentrations ([GuHCl]) ranging from 0 to 6.5 M. The first solution contained 0 M GuHCl, 2.2 μM metallopeptide, and 5 mM phosphate in the case of As(III) and 5 mM TRIS in the case of Cd(II) binding; the second solution contained 7.0 M GuHCl, 2.2 μM metallopeptide, and 5 mM corresponding buffer. The guanidinium concentration in the latter solution was determined by using refractive index measurements, as described by Pace.[41] The pH of both stock solutions was adjusted to 8.5 using NaOH. Titrations were performed in a stirred 1 cm path length strain-free rectangular cell by a Microlab 500 series automatic titrator (Hamilton Co.) controlled by an IBM computer running the CDS software supplied by AVIV. For each new point in the titration, the sample was stirred for 90 s. After this interval, 300 data points were taken at 25 °C and averaged to obtain the signal. The data were corrected for buffer contributions by subtracting a buffer blank.

For experiments using As(TRI L16C)$_3$, however, solutions containing >5.5 M GuHCl were observed to unfold irreversibly. Therefore, denaturation studies of the As(TRI L16C)$_3$ were carried out by mixing two stock solutions of differing GuHCl concentrations to generate samples ranging from 0 to 5.3 M GuHCl: stock solution 1 was 0 M GuHCl, 5 mM phosphate, and 2.2 μM As(TRI L16C)$_3$; stock solution 2 was 5.5 M GuHCl, 5 mM phosphate, and 2.2 μM As(TRI L16C)$_3$. Data points at [GuHCl] > 5.5 M were obtained by injecting 30 μL of 220 μM As(TRI L16C)$_3$ into a 2.97 mL solution containing the desired amount of GuHCl and recording the CD signal at 222 nm within 10 s of injection. Comparison of these data to those of unmetalated peptide demonstrated the ability of As to *kinetically* stabilize the three-helix bundle when [GuHCl] > 5.5 M.

NMR Spectrocopy. ^{113}Cd NMR spectra were collected on a Brucker AMX 500 spectrophotometer equipped with a 5 mm tunable broadband probe using 0.1 M $Cd(ClO_4)_2$ in D_2O as an external reference. 1-D spectra were collected using a calibrated 60° pulse (20 μs) and a sweep width of 500 ppm (55555.5 Hz) without proton decoupling. All spectra were recorded at 292 K over 3 h using 3500 scans separated by a 2 s delay. The ^{113}Cd−peptide solutions were prepared by using $^{113}CdCl_2$ (95% enriched, Cambridge Isotopes). Solutions of 2 mM concentration of the complex were prepared with rigorous purging with Ar in 10% D_2O in the absence of a buffer solution. The pH was adjusted to 8.4 with a KOH solution, and the pH was checked before and after the measurement. To generate spectra, the FID was treated with an exponential weight function using a line broadening value of 50 Hz after it was zero-filled with 32K zero points in order to increase the resolution. All spectra were generated from the FID's using the software MestRe-C.[42]

EXAFS: XAS Data Collection and Analysis. Three sets of samples containing 2 mM Cd(II) and 8 mM TRI L12C or TRI L16C at pH 5.5/8.5/9.5 and 2mM Hg with 12 mM TRI L12C or TRI L16C at pH 9.5 were independently prepared for EXAFS measurements. XAS data were collected at Stanford Synchrotron Radiation Laboratory (SSRL) on beam lines 7-3 and 9-3 for Cd and Hg samples, respectively. A Si(220) double crystal monochromator was detuned to 50% of the maximum intensity for harmonic rejection on beam line 7-3. A Rh-coated mirror upstream of the monochromator was used for harmonic rejection on beam line 9-3. The beam energy was 3 GeV, and the beam size was 1 × 10 mm^2. The X-ray energies were calibrated by collecting the absorption spectrum of a Cd foil or $HgCl_2$ references at the same time as the fluorescence data, with the first inflection points assigned as 26 714 eV (Cd) and 12 285 eV (Hg). The sample temperature was maintained between 9.8 and 12.6 K during data collection using an Oxford liquid helium flow cryostat. XAS data were collected as fluorescence excitation spectra using a 13-element (7-3) or a 30-element (9-3) Ge solid-state detector array. Spectra were measured with 10 eV increments in the pre-edge region (Cd, 26 485−26 695 eV; Hg, 12 055−12 265 eV), 1.0 eV increments in the edge region (Cd, 26 695−26 745 eV; Hg, 12 265−12 315 eV), and 0.05 Å^{-1} increments in the EXAFS region (2.75−14.00 Å^{-1}), with integration times of 1 s in the pre-edge and edge and 1−20 s (k^3-weighted) in the EXAFS region, for a total scan time of 35 min. For all samples, the first and last spectra were compared to confirm the lack of radiation damage during the measurements.

Each channel of each scan was examined for glitches. The fluorescence from the good channels was averaged for each sample to give the raw data. The raw data were normalized to the tabulated X-ray absorption coefficients[43] by using MBACK.[44] Data were converted to k space, $k = [2m_e(E - E_0)/h^2]^{1/2}$, using a threshold energy (Cd, E_0 = 26 716.3 eV; Hg, E_0 = 12 290 eV) that was calibrated by fitting the EXAFS data for the crystallographically characterized reference compounds $Cd(ClO_4)_2$ and $Cd(SC(^iPr)_3)_3^-$.[45] Background in EXAFS data was further removed by using a least-squares spline with k^3 weighting.

The EXAFS data, $\chi(k)$, were fit to eq 2 where N_s is the number of

$$\chi(k) = \sum_s \frac{N_s A_{as}(k)}{kR_{as}^2} \exp(-2\sigma_{as}^2 k^2) \sin(2kR_{as}(k) + \phi_{as}(k)) \quad (2)$$

scatterers with atom type s at a distance of R_{as}, $A_{as}(k)$ is the effective backscattering amplitude function, σ_{as}^2 is the Debye−Waller factor (disorder in R_{as}), and $\phi_{as}(k)$ is the phase-shift of the photoelectron wave traveling between the potentials of the absorbing and scattering atoms. The amplitude and phase functions, $A_{as}(k)$ and $\phi_{as}(k)$, were calculated using FEFF 7.02, with an amplitude scale factor (0.9) and the threshold energy E_o calibrated by fitting crystallographically defined model

(41) Pace, C. N.; Scholtz, J. M. In *Protein Structure: A Practical Approach*; Creighton, T. E., Ed.; Oxford University Press: Oxford, 1997; pp 299−321.
(42) Cobas, C.; Cruces, J.; Sardina, F. J. In; 2.3 ed.; Universidad de Santiago de Compostela: Santiago de Compostela, Spain, 2000.
(43) McMaster, W. H.; Del Grande, N. K.; Mallett, J. H.; Hubbell, J. H. Lawrence Livermore Radiation Laboratory, Livermore, CA, 1969.
(44) Weng, T.-C.; Waldo, G. S.; Penner-Hahn, J. E. Manuscript in preparation.
(45) Duhme, A. K.; Strasdeit, H. *Z. Anorg. Allg. Chem.* **1999**, *625*, 6−8.

complexes. Raw data were k^3-weighted, and the individual fits were performed in k space (1.5−13.0 Å^{-1}), allowing R_{as} and σ_{as}^2 to vary for each shell.[46]

Perturbed Angular Correlation. All perturbed angular correlation (PAC) experiments were performed with a setup using six detectors at a temperature of 1 ± 2 °C, which was controlled by a Peltier element. The radioactive cadmium was produced on the day of the experiment at the University Hospital cyclotron in Copenhagen and extracted as described previously,[47] except for the HPLC separation of zinc and cadmium, which was omitted in order to avoid chloride contamination of the sample. This procedure may lead to zinc contamination of the sample, but the level of contamination (a few micromolar) should not interfere with the experiment. The ^{111m}Cd solution (10−40 mL) was mixed with nonradioactive cadmium acetate and TRIS buffer. The TRI L12C or TRI L16C peptide was then added (dissolved in ion-exchanged water), and the sample was left to equilibrate for 10 min to allow for metal binding. Finally, sucrose was added to produce a 50% w/w solution, and the pH of the solution was adjusted with H_2SO_4 or KOH. To measure the pH, a small volume of sample was removed from the solution to avoid chloride contamination of the sample. [Note: The pH was measured at room temperature the following day. The pH of solutions buffered by TRIS is temperature dependent. Because of the pH dependence on the temperature of TRIS solutions, the pH of the solution at 1 °C was calculated using pH(1 °C) = 0.964[pH(25 °C)] + 0.86.][47] The samples were either used immediately after preparation or left on ice until the measurement was started. All buffers were purged with Ar and treated so as to lower metal contamination. The final volume of the samples ranged between 0.05 and 0.5 mL with concentrations of 300 μM peptide and 20 mM TRIS and a Cd(II)/peptide ratio of 3.8−12.

Results

Synthesis and Characterization of Apopeptides. The peptides used in this study are based on the parent peptide TRI, which has the sequence Ac-G(LKALEEK)$_4$G-NH$_2$ that is acetylated at the N-terminus and amidated at the C-terminus. The specific peptides used are presented in Scheme 1. The nomenclature indicates the site of replacement of a leucine by a cysteine into the TRI sequence. Both of the substitutions, TRI L12C and TRI L16C, result in the replacement of one of the leucines in the hydrophobic core of the parent peptide, TRI, with a cysteine. The substitution occurs at a *d* position in TRI L12C and at an *a* position in TRI L16C. Previous studies with TRI and cysteine-substituted TRI derivatives,[14] and a similar peptide containing alternating layers of valine and leucine, V_aL_d,[38] have confirmed that these peptides form exclusively three-stranded coiled coils above pH 7 and two-stranded coiled coils below pH 5. The X-ray structure of V_aL_d has been reported, supporting its three-stranded coiled coil structure,[48] and ^{1}H NMR investigation of TRI L12C and TRI L16C has confirmed this structural motif for the apopeptides in pH 7.5 solution.[49]

UV−Vis and CD Titrations. The formation of metal complexes with TRI L12C or TRI L16C was monitored using the ligand-to-metal charge-transfer (LMCT) bands for Cd−S or Hg−S bonds in the ultraviolet spectral window.[14] To dinstiguish these metal-centered bands from the UV absorption

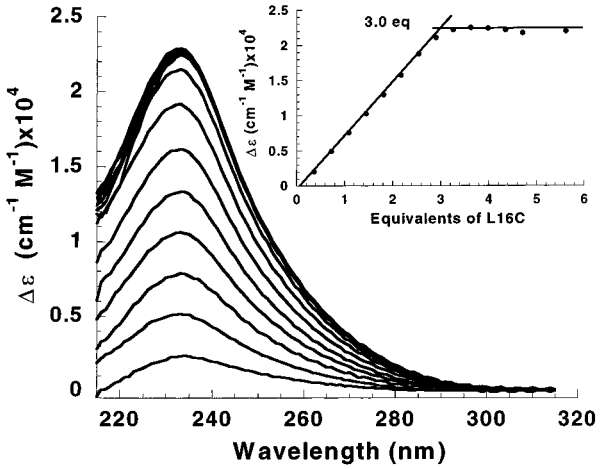

Figure 1. UV−vis titration of TRI L16C into a solution of Cd(II) at pH 8.5.The data are plotted as $\Delta\epsilon$ vs wavelength. The inset to the figure provides the titration curve plotted as $\Delta\epsilon$ at 231 nm vs equivalents of peptide added. The [Cd(II)] = 20 μM.

Table 1. Physical Parameters for Metallopeptide Complexes

peptide	UV–vis, nm ($\Delta\epsilon$)[a]	CD, nm ($\Delta[\Theta]_{222}$)[b]	EXAFS MS, Å	NMR δ, ppm
Cd(TRI L12C)$_3^-$	231 (20 600)	239 (−6) 260 (−2)	2.49	619[c]
Cd(TRI L16C)$_3^-$	232 (22 600)	238 (+26) 274 (−8)	2.49	625[c]
CdS_3^-	190−260 (15 000−25 000)		2.42−2.48	570−660[c]
Hg(TRI L12C)$_3^-$ [d]	230 (21 300) 247 (15 000) 297 (5500)	245 (+11) 275 (+2)	2.44	
Hg(TRI L16C)$_3^-$	247 (19 200) 265 (11 900) 295 (5800)		2.44	−179[d]
As(TRI L16C)$_3$			2.25	

[a] Units for extinction coefficient are M^{-1} cm^{-1}. [b] Units for molar ellipticity are deg cm^{-1} dM^{-1}. [c] ^{113}Cd NMR chemical shift reported relative to 0.1 M Cd(ClO$_4$)$_2$ in D$_2$O. Data collected at pH 8.5. [d] All data were collected at pH 8.5, except for Hg(TRI L12C)$_3^-$ (pH 9.4) unless noted otherwise. [d] ^{199}Hg NMR chemical shift reported relative to dimethyl mercury. Data collected at pH 8.[14]

of the rest of the peptide, difference spectra were taken by subtracting a background of peptide in the absence of metal. Extinction coefficients for the LMCT from these difference spectra were calculated on the basis of the total metal concentration. Figure 1 illustrates the typical difference absorption spectra for the titration of Cd(II) into a solution of TRI L16C at pH 8.5. The λ_{max} for the titration is at 232 nm with an extinction coefficient of 22 600 M^{-1} cm^{-1}. Comparable titrations of Cd(II) into TRI L12C yielded spectra that were generally similar but distinctly different, as shown by the parameters in Table 1. The titration curves for the binding of Cd(II) to either peptide, shown as an inset to Figure 1 for TRI L12C, are indicative of the development of a single species with a strong formation constant. The data are consistent with the formation of a 1:3 metal−peptide complex.

While the UV−vis spectra of the TRI L12C and the TRI L16C complexes with Cd(II) at pH 8.5 are similar, there appear to be small differences that can be magnified by observation of the transitions in the CD spectra of the two species. Figure 2a compares the difference CD spectra of the cadmium complexes of TRI L12C and TRI L16C. The spectra indicate that there are at least two significant electronic transitions between 230

(46) Clark-Baldwin, K.; Tierney, D.; Govindaswamy, N.; Gruff, E. S.; Kim, C.; Berg, J.; Koch, S. A.; Penner-Hahn, J. E. *J. Am. Chem. Soc.* **1998**, *120*, 8401.
(47) Hemmingsen, L.; Bauer, R.; Bjerrum, M.; Adolph, H.; Zeppezauer, M.; Cedergren-Zeppezauer, E. *Eur. J. Biochem.* **1996**, *241*, 546−551.
(48) Ogihara, N. L.; Weiss, M. S.; Degrado, W. F.; Eisenberg, D. *Protein Sci.* **1997**, *6*, 80−88.
(49) Gorst, C. M.; Clark-Baldwin, K.; O'Connell, J.; Pecoraro, V. Manuscript in preparation.

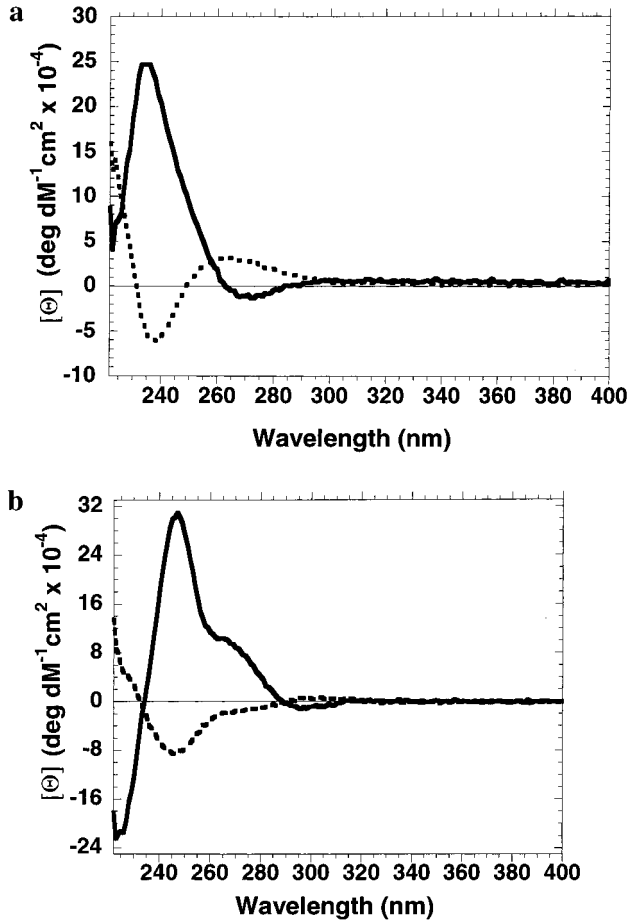

Figure 2. Comparison of the CD spectra for (top) $Cd^{II}(TRI\ L16C)_3^-$ (solid line) and $Cd^{II}(TRI\ L12C)_3^-$ (dashed line) at pH 9.4 and (bottom) $Hg^{II}(TRI\ L16C)_3^-$ (solid line) at pH 8.5 and $Hg^{II}(TRI\ L12C)_3^-$ (dashed line) at pH 9.4.

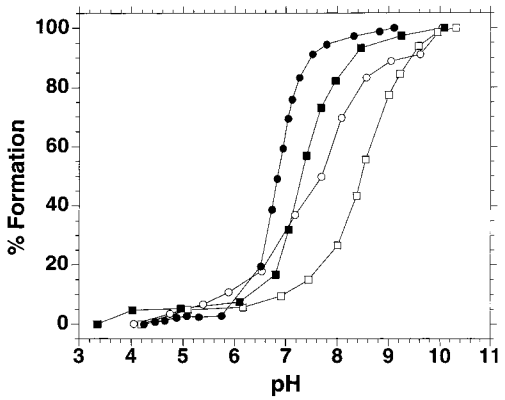

Figure 3. Comparison of the pH-dependent binding curves for Cd(II) (filled symbols) and Hg(II) (open symbols) to TRI L16C (circles) and TRI L12C (squares). The data are plotted as $\Delta\epsilon$ vs pH. The concentration of $[\{Cd^{II}\text{-}[peptide]_3\}] = 10\ \mu M$.

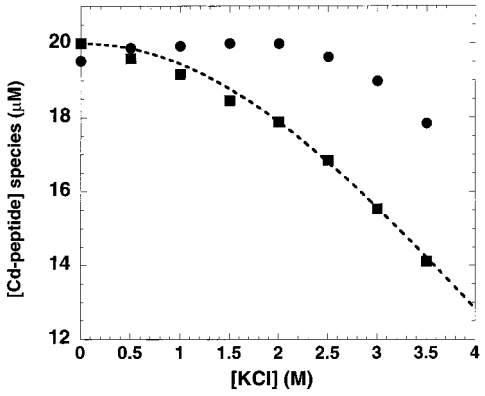

Figure 4. Plot of metal-peptide concentration vs KCl concentration for $Cd^{II}(TRI\ L16C)_3^-$ (filled circles) and $Cd^{II}(TRI\ L12C)_3^-$ (filled squares) at pH 8.5. The dashed line represents the fit to the model where Cl^- abstracts Cd(II) from the peptide assembly to form $CdCl_4^{2-}$. The dissociation constant $K_{Cdpep} = 3 \times 10^{-9}$ M is deduced from the fit of eq 6 with $K_{Cl} = 10^{1.6}\ M^{-4}$. The fit to $Cd^{II}(TRI\ L16C)_3^-$ data using the same mechanism was not satisfactory.

and 300 nm. Interestingly, the polarity of the two transitions appear to be opposite, with the band at 240 nm yielding a negative ellipticity and the one at 265 nm showing a positive ellipticity for the Cd(II):TRI L12C complex. Moreover, in comparing the LMCT bands in the Cd(II):TRI L12C complex with those of the Cd(II):TRI L16C complex, the CD signal for the LMCT transitions in the two different complexes are roughly opposite. A similar phenomenon is seen in the difference CD spectra of the Hg(II) peptides shown in Figure 2b, although in the Hg(II) spectra three possible transitions are observed.

The pH titrations of Cd(II) bound to TRI L16C and TRI L12C in Figure 3 also show differences between the two peptides. The formation of the trigonal thiolato Cd(II) complex occurs at a significantly lower pH for TRI L16C than for TRI L12C. The pK_a values that describe these differences are 6.8 for $Cd^{II}(TRI\ L16C)_3^-$ and 7.2 for $Cd^{II}(TRI\ L12C)_3^-$. Both peptides allow for complete complexation of Cd(II) by pH 8.5. When titrations of Hg(II) peptides are undertaken, a similar difference appears for trigonal thiolato Hg(II) formation as for trigonal thiolato Cd(II) formation, with the apparent pK_a for the $Hg^{II}(TRI\ L16C)_3^-$ complex being 7.8 and that for $Hg^{II}(TRI\ L12C)_3^-$ being 8.5.

GuHCl denaturation titrations were attempted with Cd(II) and As(III) in an effort to evaluate peptide stability. The titration curves for $Cd^{II}(TRI\ L12C)_3^-$ and $Cd^{II}(TRI\ L16C)_3^-$ were identical to those for the nonmetalated peptides,[38] implying that either the metal had no effect on the stability of the metal peptide complex or it was extracted before the peptide was denatured. Because of very slow kinetics of the As(III) system, individual samples were prepared in advance and then measured sequentially to evaluate the protein stability. It was found that the system was denatured after the addition of 5 M GuHCl; however, the unfolding process was irreversible. This observation indicated that the stabilization of the As(III) peptide complex is probably kinetic rather than thermodynamic.

The UV−vis spectral changes associated with the addition of KCl to solutions of $Cd^{II}(TRI\ L16C)_3^-$ and $Cd^{II}(TRI\ L12C)_3^-$ are shown in Figure 4. The spectral changes associated with the Cd(II):TRI L12C complex are more sensitive to the addition of chloride (only 36% of the signal present in the absence of chloride is present by 3.5 M KCl) than those for the Cd(II):TRI L16C complex (79% of the initial signal is still present at 3.5 M KCl). The binding of Hg(II) or As(III) by either peptide did not seem to be sensitive to chloride concentrations of 3.5 M (data not shown).

The binding equilibrium can be defined as shown with eqs 3 and 4.

$$CdP_3^- \Leftrightarrow Cd^{2+} + P_3 \qquad K_{CdPep} \qquad (3)$$

$$Cd^{2+} + 4Cl^- \leftrightarrow CdCl_4^{2-} \qquad K_{Cl} \qquad (4)$$

Dissociation constants were calculated at pH 8.5 on the basis of changes in the UV−vis spectra during the titration with KCl.

The overall equilibrium constant K_{comp} is defined as shown in eq 5, where K_{Cdpep} and K_{Cl} are the dissociation constant of eq 3 and the association constant of eq 4 respectively, CdP_3^- is $Cd^{II}(TRI\ L12C)_3^-$, and P_3 is $(TRI\ L12C)_3$.

$$K_{comp} = \frac{[P_3][CdCl_4^{2-}]}{[CdP_3^-][Cl^-]^4} = K_{Cdpep}K_{Cl} \qquad (5)$$

$$K_{CdPep} = \frac{([Cd^{2+}]_T - [CdP_3^-])([P_3]_T - [CdP_3^-])}{[CdP_3^-][Cl^-]_T^4 K_{Cl}} \qquad (6)$$

The value of K_{Cl} varies with ionic strength. $K_{Cl} = 10^{1.6}\ M^{-4}$ was selected from the reported values[50] corresponding to 3 M ionic strength. Equation 6 was solved for $[CdP_3^-]$, and the resulting equation (not shown) was used to fit the experimental data. The fit was satisfactory for K_{Cdpep}(TRI L12C) (Figure 4), and a value of 2.5×10^{-9} M was obtained. The same equation did not provide a satisfactory fit for TRI L16C, implying a more complex mechanism in this case.

^{113}Cd NMR. The coordination environment of the cadmium ion in $Cd^{II}(TRI\ L12C)_3^-$ and $Cd^{II}(TRI\ L16C)_3^-$ was probed using ^{113}Cd NMR. The ^{113}Cd NMR spectra for these two complexes at pH 8.5 are shown in Figure 5. A single resonance was observed for both solutions with chemical shifts of 619 and 625 ppm (vs 0.1 M $Cd(ClO_4)_2$ in D_2O) for $Cd^{II}(TRI\ L12C)_3^-$ and $Cd^{II}(TRI\ L16C)_3^-$, respectively. The half-height line width for both cases was measured to be 155 Hz.[51] These spectra are consistent with thiol ligation to Cd(II) and similar to those of previous model compounds with a trigonal thiolate environment (577 ppm)[52,53] and a designed helical bundle which was also reported to contain a trigonal Cd(II) thiolate coordination sphere (572 ppm).[37] Typically, ^{113}Cd NMR resonances are shifted downfield by 140−200 ppm[54] per thiolate ligand as water is substituted by thiols. Moreover, the reported chemical shifts of model compounds correspond to aromatic-thiol-containing compounds that are expected to be upfield shifted by about 40−60 ppm relative to cysteine thiols.[55,56] The chemical shifts observed for the Cd(II) complexes of TRI L12C and TRI L16C are consistent with a three-sulfur environment or a mixture of a three-sulfur environment and a higher coordination compound.

Extended X-ray Absorption Fine Structure (EXAFS) Spectroscopy. (a) Mercury X-ray Absorption Spectroscopy (XAS). We have shown previously[14] that the Hg EXAFS for a 1:2 mixture of Hg(II):L16C is consistent with a digonal mercury(II) thiolate structure. When additional peptide is added, giving a 1:3 ratio of Hg(II):L16C, the EXAFS data indicated a 0.06 Å increase in Hg−S distance, consistent with formation of a trigonal mercury(II) thiolate complex. We noted at that time that the 1:3 mixture showed an unusually large Debye−Waller factor, consistent with a highly distorted site, and that the average Hg−S distance was somewhat shorter than would be expected for a symmetric $Hg-S_3$ complex. This distortion could arise from an inherently distorted Hg environment (e.g., a T-shaped Hg site) or could reflect a heterogeneous sample, containing for example a mixture of 1:2 and 1:3 complex.

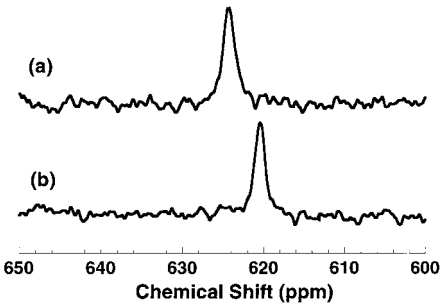

Figure 5. ^{113}Cd NMR of $Cd^{II}(TRI\ L16C)_3^-$ and $Cd^{II}(TRI\ L12C)_3^-$ at pH 8.5. Top spectrum (a) $Cd^{II}(TRI\ L16C)_3^-$ at pH 8.5; bottom spectrum (b) $Cd^{II}(TRI\ L12C)_3^-$ at pH 8.5.

Table 2. EXAFS Best-Fit Parameters

condition	sample	N_S	R_S	σ^2_S	ref
	Mercury EXAFS				
pH 5.5	1:2 Hg:L16C	2	2.324	1.4	14
pH 8.5	1:2 Hg:L16C	2	2.317	1.1	14
pH 8.5	1:3 Hg:L16C	3	2.370	10.0	14
pH 9.5	1:6 Hg:L16C	2	2.443	3.0	present
pH 9.5	1:6 Hg:L12C	2	2.400	5.8	present
solid model	$Hg(S\text{-}tBu)_3$	3	2.439	2.1	52
average of 21 models	$Hg(SR)_2$	2	2.34		75
average of 5 models	$Hg(SR)_3$	3	2.44		52, 53, 69, 76, 77
	Cadmium EXAFS				
pH 8.5	Cd−TRI L16C	3	2.493	3.2	present
pH 9.5	Cd−TRI L16C	3	2.497	2.3	present[a]
pH 8.5	Cd−TRI L12C	3	2.487	3.2	present[a]
pH 9.5	Cd−TRI L12C	3	2.498	2.3	present
solid model	$Cd(S\text{-}Trt)_3$	3	2.428	1.5	45
average of 3 models	$Cd(SR)_3$	3	2.45		45, 53, 69
average of 14 models	$Cd(SR)_4$	4	2.53		78

[a] Average of two independent measurements.

To better characterize the Hg(II)−TRI L16C interaction, we have made additional measurements, using a 1:6 Hg(II):peptide ratio. The higher peptide concentration ensures that, if there is a mixture of 1:2 and 1:3 complexes, the equilibrium will shifted toward the 1:3 complex. In addition, we have made the new measurements at pH 9.5 rather than pH 8.5. As discussed above, the three-helix coiled coil is favored at higher pH; thus, the pH 9.5 measurements should, again, favor the 1:3 complex. The EXAFS data (see Table 2) show a longer Hg−S distance and a smaller Debye−Waller factor than was found previously for the 1:3 complex. The metric parameters for the 1:6 complex are in complete agreement with the distances expected for a symmetric HgS_3 complex, suggesting that the Hg(II) forms a regular, undistorted $Hg^{II}(Cys)_3$ complex in the presence of excess TRI L16C. If we treat the average Hg−S distance for the 1:3 complex at pH 8.5 as the weighted average of the Hg−S distances in $Hg^{II}(TRI\ L16C)_2$ and $Hg^{II}(TRI\ L16C)_3$, we can use the observed Hg−S distances for the digonal and trigonal Hg−L16C complexes (2.32 and 2.44 Å) to calculate the relative

(50) Martel, A. E.; Smith, R. M. *Critical stability constants*; Plenum: New York, 1974; Vol. 5.
(51) The line width was measured from an FID dataset that was processed with a 10 Hz line-broadening function.
(52) Watton, S. P.; Wright, J. G.; Macdonnell, F. M.; Bryson, J. W.; Sabat, M.; Ohalloran, T. V. *J. Am. Chem. Soc.* **1990**, *112*, 2824−2826.
(53) Santos, R. A.; Gruff, E. S.; Koch, S. A.; Harbison, G. S. *J. Am. Chem. Soc.* **1991**, *113*, 469−475.
(54) Summers, M. F. *Coord. Chem. Rev.* **1988**, *86*, 43−134.
(55) Corwin, D. T.; Gruff, E. S.; Koch, S. A. *Inorg. Chim. Acta−Bioinorg. Chem.* **1988**, *151*, 5−6.
(56) Corwin, D. T.; Gruff, E. S.; Koch, S. A. *J. Chem. Soc., Chem. Commun.* **1987**, 966−967.

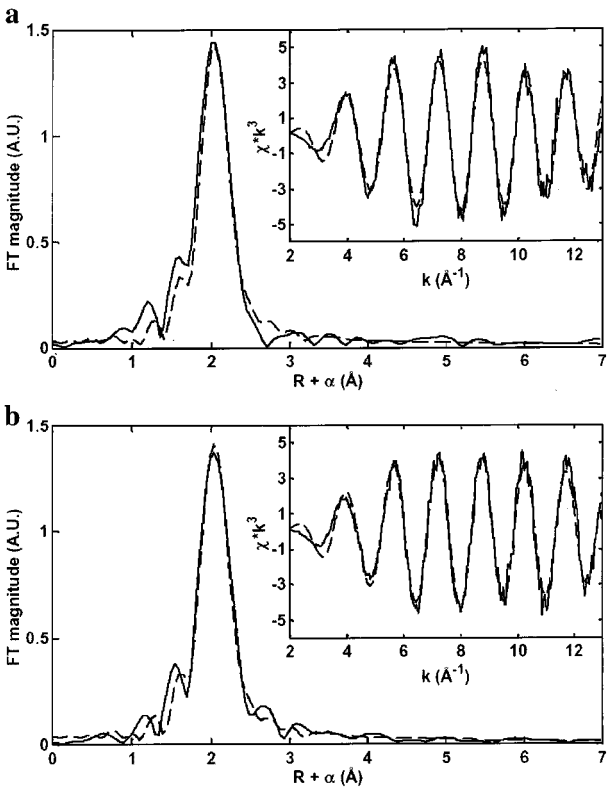

Figure 6. EXAFS data for Cd^{II}(TRI L12C) (top) and Cd^{II}(TRI L16C) (bottom) at pH 8.5. In each graph, the solid line corresponds to the experimental data and the dashed line to the fit. The insets contain the data in the *k* space before Fourier transformation.

amount of 1:2 and 1:3 complex in solution at pH 8.5. This analysis gives one-third $Hg^{II}(TRI\ L16C)_3$ and two-thirds $Hg^{II}(TRI\ L16C)_2$.[57]

In addition, we have made measurements for a 1:6 ratio of Hg(II):TRI L12C. In this case, both the average Hg−S and the apparent Debye−Waller factor are intermediate between those found for 1:3 Hg(II):TRI L16C and those found for 1:6 Hg(II):TRI L16C. This suggests that, even with a 1:6 excess of TRI L12C, the trigonal complex is not completely formed, even at pH 9.5. Using the average Hg−S distance as an indicator of composition, the observed Hg−S distance of 2.40 Å would be consistent with a 40:60 mixture of digonal and trigonal Hg. Incomplete conversion to the trigonal environment is consistent with the higher pK_a found for the TRI L12C peptide.

(b) Cadmium XAS. The normalized Cd XANES spectra (see Supporting Information) are identical for Cd^{II}(TRI L12C) and Cd^{II}(TRI L16C) at pH 8.5, indicating that the Cd(II) environment must be very nearly identical in both peptides. Identical spectra (not shown) are found for samples prepared at pH 9.5. The XANES spectra for Cd^{II}(TRI L12C) and Cd^{II}(TRI L16C) at pH 5.5 are likewise very similar. However, the spectra at pH 5.5 are dramatically different from those at higher pH, indicating a significant change in structure as the pH is lowered.

The EXAFS data $Cd^{II}(TRI\ L12C)_3^-$ and $Cd^{II}(TRI\ L16C)_3^-$ at pH 8.5 are shown in Figure 6. In both cases, the Fourier transforms of the EXAFS data give a single narrow peak, suggesting a homogeneous ligation environment. Nearly identical Fourier transforms (not shown) are found for data measured at higher pH. The best fit to the k^3-weighted EXAFS data (shown as the dashed line) was obtained using three sulfur atoms at a distance of 2.49 Å with a Debye−Waller factor of (2.5−3.8) $\times 10^{-3}$ Å^2. Identical metric parameters were obtained for both peptides. If an oxygen shell is introduced into the fits, there is negligible improvement in the fit quality, and the oxygen shell refines to an unrealistically large Debye−Waller factor (0.010 Å^2), demonstrating that the data do not represent a stoichiometric CdS_3O ligation environment. The EXAFS data are thus consistent with exclusively sulfur ligation to the Cd, although they do not allow us to rule out the presence of a small population of low-Z scatterers (e.g., oxygen or nitrogen).

Perturbed Angular Correlation (PAC) Spectroscopy. Perturbed angular correlation spectroscopy was used to determine the cadmium coordination geometry within the coiled coils formed by TRI L12C and TRI L16C. A brief overview of PAC will be given here because it is not a frequently encountered technique. More thorough descriptions of the technique are provided in a review by Frauenfelder and Steffen,[58] and the biological applications are described in a review by Bauer.[59] Other descriptions and specific examples of applications are also available.[47,60−63]

Radioactive ^{111m}Cd decays by successive emission of two γ rays. They are emitted anisotropically, meaning the second γ ray is emitted in a nonrandom direction with respect to the first. If the nucleus interacts with an electric field gradient of its surroundings, the intermediate nuclear level is split, perturbing the angular correlation of the emitted γ rays. In ^{111m}Cd PAC spectroscopy, this splitting is quantified. There are three energy differences that can be measured using ^{111m}Cd PAC spectroscopy. Only two of these energy differences are independent; the third is the sum of the first two. For samples of identical, static, and randomly oriented molecules, the perturbation function is given by eq 8.

$$G_2(t) = a_0 + a_1 \cos(\omega_1 t) + a_2 \cos(\omega_2 t) + a_3 \cos(\omega_3 t) \quad (8)$$

The analogue of this function (multiplied by the total amplitude, *A*, see below), derived from experimental results with the Cd:TRI L12C and Cd:TRI L16C systems, is given in Figure 7, along with their Fourier transforms. Two parameters, ω_o and η, can be determined from the data.[64] Roughly speaking, ω_o is associated with the strength of the interaction between the surrounding electronic environment and the Cd nucleus, and η is associated with the asymmetry of the interaction. η is always between 0 and 1, with a value of 0 when there is axial symmetry. These two parameters are defined as

(57) We also use a linear combination of EXAFS data from $Hg^{II}(TRI\ L16C)_2$ at pH 5.5 and $Hg^{II}(TRI\ L16C)_3^-$ at pH 9.5 to fit the data and have similar results.

(58) Frauenfelder, H.; Steffen, R. In *Alpha-, Beta- and Gamma-ray spectroscopy*; Siegbahn, K., Ed.; North-Holland, Amsterdam, 1965; Vol. 2, pp 997−1198.
(59) Bauer, R. *Q. Rev. Biophys.* **1985**, *18*, 1−64.
(60) Hemmingsen, L.; Bauer, R.; Bjerrum, M.; Zeppezauer, M.; Adolph, H.; Formicka, G.; Cedergren-Zeppezauer, E. *Biochemistry* **1995**, *34*, 7145−7153.
(61) Bauer, R.; Danielsen, E.; Hemmingsen, L.; Sorensen, M.; Ulstrup, J.; Friis, E.; Auld, D.; Bjerrum, M. *Biochemistry* **1997**, *36*, 11514−11524.
(62) Danielsen, E.; Scheller, H.; Bauer, R.; Hemmingsen, L.; Bjerrum, M.; Hansson, O. *Biochemistry* **1999**, *38*, 11531−11540.
(63) Paul-Soto, R.; Zeppezauer, M.; Adolph, H.; Galleni, M.; Frere, J.; Carfi, A.; Dideberg, O.; Wouters, J.; Hemmingsen, L.; Bauer, R. *Biochemistry* **1999**, *38*, 16500−16506.
(64) Each plot contains two separate sets of three transitions.

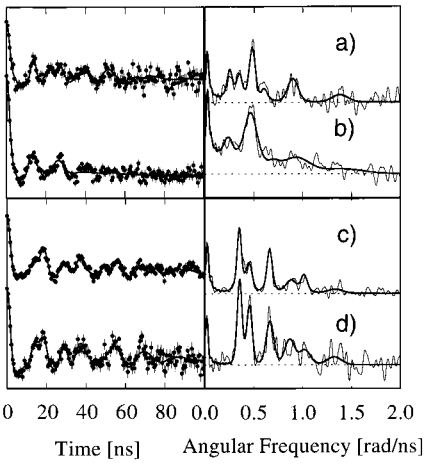

Figure 7. (Left) Perturbation function (experimental data are shown as filled circles with error bars, fit shown as full line) and (right) the Fourier transform (the thin line gives the Fourier transform of the experimental data, and the thick line gives the Fourier transform of the fit). (a) TRI L12C peptide at a peptide:Cd ratio of 3.8:1; (b) TRI L12C peptide at a peptide:Cd ratio of 12:1; (c) TRI L16C peptide at a peptide:Cd ratio of 3.8:1; (d) L16C peptide at a peptide:Cd ratio of 12:1.

$$\omega_0 = 12\pi|V_{zz}\,\mathrm{eQ}|/(40h) \qquad \text{and} \qquad \eta = (V_{xx} - V_{yy})/V_{zz}$$

where eQ is the electric quadrupole moment of the cadmium nucleus in the intermediate state, h is Planck's constant, and V_{ii} are the eigenvalues of the electric field gradient tensor, conventionally ordered so that $|V_{zz}| \geq |V_{yy}| \geq |V_{xx}|$. Three additional parameters are important in interpreting the PAC spectra and are deduced from the data. The first, $\Delta\omega_o/\omega_o$, is used to describe a Gaussian frequency distribution centered at ω_o. This value is a measure of small geometric variations in the coordination geometry of cadmium from peptide to peptide in the same solution, not including changes in number or types of ligands. The second, τ, is a measure of the rotational correlation time of the Brownian tumbling and other dynamic features of the proteins in solution. These parameters generally describe geometrical perturbations or fluctuations of the ligands. Sucrose is added to the samples in order to reduce the rotational diffusion. The third parameter, A, is the amplitude of the signal. If there is more than one set of signals in the spectrum, each set of signals has to be modeled using a separate set of parameters (ω_o, η, $\Delta\omega_o/\omega_o$, τ, and A).

To derive the coordination geometry from the PAC data for complexes of cadmium with TRI L12C and TRI L16C given in Table 3 (best-fit parameters), we applied a semiemperical angular overlap model (AOM).[65] The AOM calculations have been estimated to deviate from experiment by about 0.030 rad/ns for ω_o.[66] The average deviation for η is harder to assess, because it will be relatively large for small ω_o. Table 4 shows the calculated values of the spectral parameters ω_o and η for a number of different ideal coordination geometries involving cysteinates and water molecules.

In all of the experimental spectra, there is a set of signals corresponding to ω_o around 0.450 rad/ns and a relatively low η between 0.12 and 0.24. This set of signals is more prominent in the experiments with a peptide:Cd(II) ratio of 12:1 than in the experiments with a peptide:Cd(II) ratio of 3.8:1. In addition, a second set of signals is observed in the spectra of both TRI L12C and TRI L16C with cadmium. This second signal is not the same for the two peptides. In the spectrum of TRI L16C, the second signal corresponds to an ω_o of 0.336 rad/ns and an η of 0.22. The minor differences between the two experiments with the TRI L16C peptide may be caused by the different pH values of the solutions. For the case of TRI L12C, this second signal appears to be different in the two spectra. As can be seen from a comparison of the values derived from the data (Table 3) and values calculated (Table 4), an ω_o of 0.45 rad/ns corresponds to a trigonal thiolate environment about the cadmium. Therefore, this set of signals can be attributable to cadmium bound to three thiolates, supporting a $Cd^{II}(Cys)_3^-$ coordination environment. The deviations of the experimental spectra from the calculated values for ω_o and η may be due to slight deviations from the planar trigonal structure, or to other small differences between the actual structure and the idealized models used to calibrate the AOM.

It is clear that a second signal is present in the data of both TRI L12C and TRI L16C. This other signal might be a distorted trigonal pyramidal $[Cd^{II}(Cys)_3]^-$ structure for the TRI L16C peptide and a distorted trigonal planar + apical water molecule $[Cd^{II}(Cys)_3(H_2O)]^-$ structure for the TRI L12C peptide. Further studies of pH effects and local dynamics at the metal ion binding sites may provide additional important information and clarify the origin of the other species. The fit of the TRI L12C 12:1 peptide:Cd spectrum is not completely satisfactory, as reflected by both the larger χ_r and its qualitative comparison with the fit (see Figure 7). The relatively high values of $\Delta\omega_0/\omega_0$ and $1/\tau$, combined with the fact that the second peak (around 0.900 rad/ns) is almost missing, strongly suggest that local dynamics at the metal ion binding site is affecting the spectra.

Discussion

We have initiated a program to design small metallopeptide aggregates that may provide versatile coordination options to metals in an effort to understand the factors that lead to stable metalloproteins. Specifically, we have been interested in designing peptide aggregates that are capable of the following objectives: (1) enforcing a higher coordination number on a metal than is observed under normal conditions in aqueous solution; (2) enforcing a lower coordination number on a metal than is observed under normal conditions in aqueous solution; and (3) controlling peptide aggregation state using metal coordination preference (e.g., two-stranded vs three-stranded α-helical bundle). As will be described below, the TRI peptide family allows us to achieve each of these objectives.

Using the TRI family of peptides, we have previously described systems that accomplish the first and third objectives.[14,38] This family of peptides has a two- to three-helix bundle transition at pH 5.5 in the absence of metal, with two-helix bundles dominating at low pH. To address the first objective, trigonal thiolato coordination was imposed upon Hg(II) with TRI L16C at high pH under conditions where Hg(II) prefers linear coordination by simple thiolates. Surprisingly, TRI L12C was not observed to stabilize trigonal thiolato Hg(II) under similar conditions (pH 8). To address the third objective, the three-helix bundle form of both TRI L12C and TRI L16C, which prefers a two-stranded coiled coil conformation at low pH, could

(65) Bauer, R.; Jensen, S.; Schmidt-Nielsen, B. *Hyperfine Interact.* **1988**, *39*, 203−234.
(66) Hemmingsen, L.; Ryde, U.; Bauer, R. *Z. Naturforsch.* **1999**, *54a*, 422−430..

Table 3. Parameters Fitted to the PAC Data

	peptide:Cd	pH	ω_0 (rad/ns)	η	$\Delta\omega_0/\omega_0$ (×100)	$1/\tau$ (ps^{-1})	A (×100)	χ_r
TRI L12C	3.8:1	8.75	0.454 ± 0.004	0.24 ± 0.02	5.5 ± 0.8	6 ± 3	3.8 ± 0.4	1.14
			0.188 ± 0.003	0.61 ± 0.04	2.0 f[a]	29 ± 8	2.9 ± 0.6	
TRI L12C	12:1	8.32	0.468 ± 0.009	0.12 ± 0.10	13.4 ± 1.7	15 ± 5	6.2 ± 0.6	1.22
			0.233 ± 0.008	0.25 ± 0.12	2.0 f[a]	81 ± 11	4.9 ± 0.8	
TRI L16C	3.8:1	8.60	0.443 ± 0.004	0.14 ± 0.04	5.6 ± 0.9	9 ± 4	2.0 ± 0.2	1.06
			0.335 ± 0.001	0.22 ± 0.01	2.2 ± 0.5	19 ± 3	4.3 ± 0.3	
TRI L16C	12:1	8.71	0.438 ± 0.004	0.20 ± 0.03	5.4 ± 0.7	3 ± 3	3.6 ± 0.4	1.10
			0.337 ± 0.002	0.23 ± 0.02	5.1 ± 0.7	8 ± 5	5.1 ± 0.6	

protein examples	coordination geometry	ω_0 (rad/ns)	η
LADH[79,80]	2 Cys, His, H_2O	0.270	0.94
CPA[81,82]	2 His, H_2O Glu (bidentate)	0.156	0.29
SOD[83,84]	3 His, H_2O	0.114	0.47
azurin[85]	2 His, Cys[b]	0.338	0.52

[a] Fixed in the fit. Changing this parameter from 0.002 to 0.2 changed the reduced χ^2 by less than 0.05. See the text for an explanation of the parameters. [b] A sulfur from Met121 and an oxygen from the amide bond carboxylate of Gly45 are also near cadmium in azurin, so it can be consider to be in a distorted trigonal bipyramid with very long axial ligands.

Table 4. Calculated PAC Parameters Using an Angular Overlap Model (AOM)

geometry	model structure	ω_0 (rad/ns)	η
$[Cd(Cys)_3]^-$	trigonal planar	0.450	0
$[Cd(Cys)_2H_2O]$	trigonal planar	0.404	0.35
$[Cd(Cys)(H_2O)_2]^+$	trigonal planar	0.357	0.39
$[Cd(Cys)_3]^-$	trigonal pyramidal	0.300	0
$[Cd(Cys)_3(H_2O)]^-$	trigonal planar + apical water molecule	0.243	0
$[Cd(Cys)_3(H_2O)]^-$	tetrahedral	0.093	0
$[Cd(Cys)(H_2O)_3]^+$	tetrahedral	0.093	0
$[Cd(Cys)_2(H_2O)_2]$	tetrahedral	0.093	1
$[Cd(Cys)_3(H_2O)_2]^-$	trigonal bipyrimidal (apical waters)	0.036	0
$[Cd(Cys)_2(H_2O)_3]$	trigonal bipyrimidal (apical cysteinates)	0.289	0
$[Cd(Cys)_2(H_2O)_4]$	octahedral	0.194	0

be stabilized at low pH (pH 2.5) by addition of As(III). The resulting As−peptide complexes were shown to have a 3:1 peptide:As(III) stoichiometry by mass spectrometry. Thus, arsenic could be used to control the peptide aggregation, satisfying this objective.

Given these successes, we felt that our design would also satisfy our final objective, imposing a lower coordination number on a metal. We believed that the sterically demanding layers of leucine that sandwich the metal binding cavity would inhibit the formation of metal centers with coordination that requires nonplanar geometries (tetrahedral, octahedral, etc.). The ideal metal to test this hypothesis is Cd(II). Like As(III) and Hg(II), Cd(II) is thiophilic; however, the chemistry of Cd(II) is dominated by compounds with coordination number 4 or greater with simple thiolate ligands.[67] Prior to the initiation of these studies, the only well-defined trigonal Cd(II) species were those prepared from organic solvents with very bulky alkyl- and arylthiolates.[45,68,69] While we were completing these studies, a report appeared of a three-stranded α-helical bundle that bound Cd(II) using an alternative peptide design, $[Cd^{II}(IZ\text{-}AC)_3]^-$, which retained the thiolate environment that was used in the TRI L16C peptide (that is, an "a" residue substitution).[37] The primary mechanism for the characterization of this complex was a ^{113}Cd chemical shift at 572 ppm and the absence of broadening of this peak when H_2O was substituted with D_2O. Thus, the assignment of a trigonal Cd(II) was tentative. These workers also found that their peptide bound Hg(II) in a manner analogous to TRI L16C.

The addition of $CdCl_2$ to a solution of TRI L16C maintained at pH 8.5 was accompanied with the absorption increase in the ultraviolet region of the spectrum shown in Figure 1. The absorption maximum of the difference spectra was centered at 232 nm, with an extinction coefficient of 22 600 M^{-1} cm^{-1}. The titration curve, shown as an inset in Figure 1, indicates that the stoichiometry of peptide to metal is 3:1. Thus, the best description for the complex is $[Cd^{II}(TRI\ L16C)_3]^-$. While this behavior might be expected on the basis of our previous studies on TRI L16C with Hg(II) and As(III), the ability of TRI L12C to bind cadmium in a trigonal environment was less certain. Nonetheless, a titration using TRI L12C gave a difference absorption maximum at 231 nm, with an extinction coefficient equal to 20 600 M^{-1} cm^{-1} (Supporting Information, Figure S1). Similarly, the titration curve provided a 3:1 peptide-to-metal stoichiometry for the Cd(II):TRI L12C complex.

While the electronic spectra are similar in energy and intensity, we noticed that the circular dichroism of the metalated peptides had subtle but reproducible differences, as shown in Figure 2. The difference CD spectrum of $Cd^{II}(TRI\ L16C)_3^-$ and TRI L16C shows a maximum at 238 nm (∼ +26 deg cm^2 dM^{-1}), a zero crossing at 263 nm, and negative ellipticity at 274 nm (∼ −8 deg cm^2 dM^{-1}). In contrast, the difference CD spectrum of $Cd^{II}(TRI\ L12C)_3^-$ is essentially inverted. The λ_{min} is −6 deg cm^2 dM^{-1} at 239 nm, with a broad positive maximum at 260 nm (−2 deg cm^2 dM^{-1}). A similar effect is seen when Hg(II) is bound to TRI L16C. In this case, the CD spectrum of $Hg^{II}(TRI\ L16C)_3^-$ has a positive maximum at 248 nm (∼ +32 deg cm^2 dM^{-1}), a weaker positive absorption at 268 nm (∼ +11 deg cm^2 dM^{-1}), and a very negative ellipticity at 300 nm (∼ −2 deg cm^2 dM^{-1}). These transitions originate from the intense LMCT excitations that are oriented because of the chiral environment of the metal binding pocket. The two-coordinate forms of $Hg^{II}(TRI\ L16C)_2$ and $Hg^{II}(TRI\ L12C)_2$ do not have significant LMCT excitations for $\lambda \geq 240$ nm, and therefore the CD spectrum for these compounds is featureless in this region. The differences in the spectra of $Cd^{II}(TRI\ L12C)_3^-$ and $Cd^{II}(TRI\ L16C)_3^-$, as well as the difference in

(67) Holloway, C. E.; Melnik, M. *Main Group Met. Chem.* **1995**, *18*, 451−585.
(68) Tang, K. L.; Jin, X. L.; Li, A. Q.; Li, S. J.; Li, Z. F.; Tang, Y. Q. *J. Coord. Chem.* **1994**, *31*, 305−320.
(69) Gruff, E. S.; Koch, S. A. *J. Am. Chem. Soc.* **1990**, *112*, 1245−1247.

the Hg(II) binding properties of TRI L12C and TRI L16C, support the contention that the environments around the metal binding site in TRI L12C and TRI L16C are different.

These observations have implications on the use of CD spectroscopy as a technique for assessing metalloprotein structure and stability. In such experiments, we see that complexes with intense metal-associated UV signatures can contribute to the CD component due to the protein. It is, therefore, necessary to address the question of whether the spectral differences observed are due to metal complexes or protein structure perturbation.

To further characterize Cd(II) binding, ^{113}Cd NMR spectra were measured. The chemical shifts at 619 ppm (Cd^{II}(TRI L12C)$_3^-$) and 625 ppm (Cd^{II}(TRI L16C)$_3^-$) are within the range of values that are reported for $Cd^{II}(SR)_3^-$ complexes.[53] They also reveal differences between Cd^{II}(TRI L12C)$_3^-$ and Cd^{II}(TRI L16C)$_3^-$ (Figure 5). However, both are shifted somewhat downfield from the 572 ppm signal reported for $Cd^{II}(IZ\text{-}AC)_3^-$, which could indicate the presence of a fourth ligand on Cd^{II}-(TRI L12C)$_3^-$ or Cd^{II}(TRI L16C)$_3^-$. The half-height line width of 155 Hz measured for both peaks is within the range of 82−287 Hz that has been reported for metallothionins[70] and broader than what has been observed for model compounds (4−47 Hz).[54]

To obtain structural evaluation of the Cd(II) site in Cd^{II}(TRI L12C)$_3^-$ and Cd^{II}(TRI L16C)$_3^-$, we collected perturbed angular correlation spectroscopic data for both of these peptides. Perturbed angular correlation spectroscopy is particularly well suited for providing angular information that would help us to assess whether the Cd(II) is trigonal planar or trigonal pyramidal, or has a loosely bound fourth ligand. In these measurements, the 3Cys trigonal planar structure is expected to give spectral parameters very different from those of trigonal pyramidal and tetrahedral structures, as seen in Table 4. The spectra of both Cd^{II}(TRI L12C)$_3^-$ and Cd^{II}(TRI L16C)$_3^-$ have a significant component which is very close to that expected for the 3Cys trigonal planar structure (ω_0 around 0.450 rad/ns and low η), see Table 3. This very high value of ω_0 is, to the best of our knowledge, the highest ω_0 reported from ^{111m}Cd PAC spectroscopy on proteins. It is very difficult to envisage a coordination geometry other than the 3Cys trigonal planar structure giving rise to this signal in a protein, a fact underlined by the examples of PAC data from selected proteins shown in Table 3. In addition, there is another component in the spectra that differs between the two TRI peptides. These components may involve higher coordination numbers and coordination by water molecules, but further experiments are necessary to elucidate this. The fact that two signals are observed in the ^{111m}Cd PAC spectra but only one in the ^{113}Cd NMR spectra indicates that the latter is due to fast exchange (on the ^{113}Cd NMR time scale) between the two coordination geometries causing the two ^{111m}-Cd PAC signals. In a recent publication it was demonstrated that ^{111m}Cd PAC and ^{113}Cd NMR spectroscopy can monitor dynamics on different time scales.[71] This agrees well with the observation that the ^{113}Cd signal for TRI L12C is affected by the presence of chloride and thus may involve coordination of water.

Further structural evaluation of the Cd(II) site in Cd^{II}(TRI L12C)$_3^-$ and Cd^{II}(TRI L16C)$_3^-$ was possible with the collection of X-ray absorption data on these metallopeptides at pH 8.5, where titration data indicated that the cadmium was completely bound by three thiolate sulfur atoms. The EXAFS data for the 1:4 Cd(II):peptide samples gave an average bond length of 2.49 Å. This distance is close, but not identical, to the Cd−S distance that is expected for CdS_3 ligation. The average Cd−S distances in CdS_3 models range from 2.42 to 2.48,[45,53,69] with an average value of 2.45. The Cd−S distance in Cd(II)−(TRI L12C) and Cd(II)−(TRI L16C) is thus longer than expected for CdS_3 but significantly shorter than the Cd−S distances (2.51−2.56 Å, average = 2.53 Å)[72] found for four-coordinate $Cd(SR)_4$ complexes. The most likely interpretation of these data is that, as for Hg(II) with TRI L12C, Cd(II) complexes are heterogeneous.

This heterogeneity is supported by the PAC results, which show that two different Cd species are present in solution; however, the behavior is dependent on whether TRI L12C or TRIL16C complexes are examined. For the Cd^{II}(TRIL12C)$_3^-$, one of the species has PAC parameters consistent with a symmetric CdS_3 site (ω_o = 454 rad/ns, η = 0.24) and accounts for approximately half of the Cd(II). The other species has PAC parameters that are consistent with a distorted Cd site(ω_o = 0.188 rad/ns, η = 0.61). While the species assigned to the trigonal CdS_3 chromophore is similar for Cd^{II}(TRI L16C)$_3^-$ (ω_o = 0.443 rad/ns, η = 0.14), the second species has different PAC parameters from the TRI L12C complex (ω_o = 0.335 rad/ns, η = 0.22). Given the observation that the EXAFS Cd−S distance is longer than expected for both peptide CdS_3 sites, the second Cd species is presumably a high-coordinate Cd complex, since this would give a longer average Cd−S distance. Since additional thiolate ligands are not available, we believe that a putative four-coordinate species most likely results from coordination of a solvent molecule. This would give rise to a small Cd−O signal in the EXAFS. However, as we have shown previously for Zn EXAFS,[73] it is extremely difficult to demonstrate the presence of a small, nonintegral fraction of low-Z ligation in the presence of high-Z scatterers. The observed Cd−S distances are consistent with an approximately 50:50 mixture of CdS_3 and CdS_3O, and this ratio is in good agreement with the amplitudes found by PAC. The EXAFS Cd−S distance is slightly, but consistently, shorter for TRI L12C than for TRI L16C. If variations in Cd−S distance are attributed solely to variations in the ratio of CdS_3 to CdS_3O species, the EXAFS distances suggest that there should be slightly more of the trigonal species for TRI L12C than for TRI L16C. This is consistent with the PAC integrations showing ca. 55% trigonal for TRI L12C but only ca. 40% trigonal for TRI L16C. In conclusion, the data demonstrate that three-coordinate trigonal planar cadmium coordination geometries do exist for both TRI peptides, but there is also another component in the system that may include the incorporation of a fourth ligand or perturbation from the trigonal structure.

At this point, we were faced with a significant observation: the cadmium binding sites are spectroscopically similar, and yet distinct. This suggested that the pH stability of Cd^{II}(TRI

(70) Vašák, M.; Hawkes, G.; Nicholson, J.; Sadler, P. *Biochemistry* **1985**, *24*, 740−747.
(71) Hemmingsen, L.; Damblon, C.; Antony, J.; Jensen, M.; Adolph, H. W.; Wommer, S.; Roberts, G. C. K.; Bauer, R. *J. Am. Chem. Soc.* **2001**, *123*, 10329−10335.
(72) See Supporting Information.
(73) Clark-Baldwin, K.; Tierney, D. L.; Govindaswamy, N.; Gruff, E. S.; Kim, C.; Berg, J.; Koch, S. A.; Penner-Hahn, J. E. *J. Am. Chem. Soc.* **1998**, *120*, 8401−8409.

$L12C)_3^-$ and $Cd^{II}(TRI\ L16C)_3^-$ might differ. To test this hypothesis, we completed pH titrations of the peptide using the UV absorption band to monitor the presence of the Cd(II) peptide complex. Figure 3 shows pH titrations of $Cd^{II}(TRI\ L12C)_3^-$ and $Cd^{II}(TRI\ L16C)_3^-$. The observed pK_a's for $Cd^{II}(TRI\ L12C)_3^-$ and $Cd^{II}(TRI\ L16C)_3^-$ are 7.2 and 6.8, respectively. Below pH 6, neither peptide appears to bind Cd(II) based on the absence of a LMCT band in the UV spectra, low, broad, chemical shifts in ^{113}Cd NMR titrations ($\delta = +14$ ppm), and no significant Cd−S interactions in perturbed angular correlation measurements (vide infra). This observation is in contrast to Hg(II) and As(III), which at low pH form $Hg^{II}(TRI\ L16C)_2$ and $As^{III}(TRI\ L16C)_3$, respectively.

We can draw two conclusions from these electronic spectra. First, the TRI L12C peptide is competent to make a trigonal planar Hg(II) complex; however, to do so requires a significant elevation in pH as compared to the case for TRI L16C. Since the thiolate pK_a's for $(TRI\ L16C)_3$ and $(TRI\ L12C)_3$ are the same, the different pH behavior for metal binding is a direct reflection of the decreased tendency of TRI L12C to form a trigonal thiolate complex. We believe that this difference is due to an approximately 1−2 kcal/mol energy penalty to perturb cysteine from its desired rotamer to form the trigonal complex. Second, the previously published spectral values for $Hg^{II}(TRI\ L16C)_3^-$, while correct for pH 8.5, underestimated the extinction coefficient for a trigonal mercury(II) tris(thiolato) complex by approximately 7%. The appropriate values for this complex are 247 nm (19 200 $M^{-1}\ cm^{-1}$), 265 nm (11 900 $M^{-1}\ cm^{-1}$), and 295 nm (5800 $M^{-1}\ cm^{-1}$). These values are in excellent agreement with the spectral parameters reported for the trigonal thiolate Hg(II) site in the mercury-sensing protein MerR,[69] which are 242 nm (19 800 $M^{-1}\ cm^{-1}$), 260 nm (14 600 $M^{-1}\ cm^{-1}$), and 295 (6450 $M^{-1}\ cm^{-1}$).

Intrigued by the substantially different apparent pK_a values for Cd(II) binding to our peptides, we decided to reinvestigate Hg(II) binding to TRI L12C.[14] Previous studies had suggested that $Hg^{II}(TRI\ L16C)_3^-$ could be formed at pH 8.5; however, similar experiments with TRI L12C gave only $Hg^{II}(TRI\ L12C)_2$. We first completed the pH titration of Hg(II) with TRI L16C, as shown in Figure 3. The apparent pK_a for this complexation is 7.8, with the conversion being between the two-coordinate $Hg^{II}(TRI\ L16C)_2$ and $Hg^{II}(TRI\ L16C)_3^-$. When a pH 4 solution of $Hg^{II}(TRI\ L12C)_2$ which contained an extra equivalent of TRI L12C was progressively made more basic, the electronic spectra indicative of $Hg^{II}(TRI\ L12C)_3^-$ developed above pH 8.0. Complex formation was complete by pH 10, yielding an apparent pK_a for the complexation of 8.6. A titration of TRI L12C into a solution of Hg(II) that was maintained at pH 9.4 (Figure S2) showed break points at 1.8 and then 3.2 equiv of added peptide. This illustrates that the $Hg^{II}(TRI\ L12C)_2$ complex is initially the stable complex but that, upon addition of a third peptide equivalent, a trigonal planar Hg(II) in a three-stranded α-helical bundle can be formed. We then collected the CD spectrum of $Hg^{II}(TRI\ L12C)_3^-$, shown in Figure 2. Just as was seen for the Cd(II) peptides, the CD spectrum of the TRI L12C derivative was inverted from that of the TRI L16C metalated bundle. Since we observed that higher pH conditions stabilize the complexes, we prepared samples for EXAFS at pH 9.5 for Hg(II) and Cd(II) with TRI L12C and TRI L16C. The distances measured in the cases of both Cd(II) samples were the same as those measured at pH 8.5. However, the distance measured for $Hg^{II}(TRI\ L16C)_3^-$ was 2.44 Å, and it was 2.40 Å for $Hg^{II}(TRI\ L12C)_3^-$. The distance for $Hg^{II}(TRI\ L16C)_3^-$ is longer than the one reported previously[14] and is now in very good agreement with the expected value for a trigonal site. We speculate that the reason for that is that the previous measurement was made on a sample that contained a mixture of both $Hg^{II}(TRI\ L16C)_2$ and $Hg^{II}(TRI\ L16C)_3^-$. The distance for $Hg^{II}(TRI\ L12C)$ at the same pH was also a little shorter than that observed for $Hg^{II}(TRI\ L16C)_3^-$. The best fit to the data indicates that there is a mixture of 60% $Hg^{II}(TRI\ L12C)_3^-$ with a distance of 2.44 Å and 40% $Hg^{II}(TRI\ L12C)_2$ with a distance of 2.30 Å. This agrees well with the discrepancy between the distances measured for $Hg^{II}(TRI\ L16C)_3^-$ that was prepared at pH 8.5 and the same sample prepared at pH 9.5. We believe that a sample of $Hg^{II}(TRI\ L12C)_3^-$ prepared at a pH 10.5 would be homogeneous and exhibit a distance of 2.44 Å.

Our next goal was to examine the stability of the system. To do that, we attempted to use guanidinium denaturations. For the TRI peptide family at room temperature and pH 8.5, the half-denaturation points occur at 3.8, 2.0, and 1.8 M for $(TRI)_3$, $(TRI\ L16C)_3$, and $(TRI\ L12C)_3$, respectively.[38] However, the denaturation titrations of $Cd^{II}(TRI\ L12C)_3^-$ and $Cd^{II}(TRI\ L16C)_3^-$ were indistinguishable from those of $(TRI\ L12C)_3$ and $(TRI\ L16C)_3$ alone. Although this could indicate that the presence of cadmium does not affect bundle stability, it is more likely that the equilibrium that is being assessed is a consequence not simply of the guanidinium cation dehydrating the peptide surface but also of the chloride ion's ability to effectively remove the cadmium ion from the bundle.

To test the hypothesis of the metal extraction, we wanted to examine the effect of Cl^- on the metal−peptide complex. That was done by monitoring the UV signatures of $Cd^{II}(TRI\ L12C)_3^-$ and $Cd^{II}(TRI\ L16C)_3^-$ at pH 8.5 while increasing the KCl concentration. As shown in Figure 4, it was found that KCl had a very large effect on the stability of the complex. Also, the two peptides showed different behavior, with the LMCT transitions for $Cd^{II}(TRI\ L16C)_3^-$ being essentially unaffected up to 2.5 M and the intensity of the charge-transfer transitions beginning to decrease above that. $Cd^{II}(TRI\ L12C)_3^-$ is clearly much more sensitive to added chloride, as shown by the progressive decrease in the 231 nm absorption from 0 to 3.5 M KCl, leaving only 34% of the signal by that time.

The Cl^- titration data can be used for a quantitative analysis of the binding constant; however, since the exact effects of Cl^- on the system are not known, the reported values should be considered more as good estimates of the binding affinity. We tried to fit the data with a simple mechanism where Cl^- extracts Cd(II) from the helical bundle and forms $CdCl_4^{2-}$. This model gave a good fit for Cd(II) binding to TRI L12C with a dissociation constant of 3×10^{-9} M (Figure 4). Metal extraction from TRI L16C appeared more complicated, so a quantitative assessment was not undertaken. It is safe to say that the binding constant in the case of TRI L16C is higher than that for TRI L12C.

If the chloride were binding to Cd(II) without displacing the thiolate ligands, one would expect a shift of the LMCT. Instead, we observed that these transitions are diminished not shifted, supporting the proposal that the Cd(II) is removed from the peptide. These data further show that, at least in competition

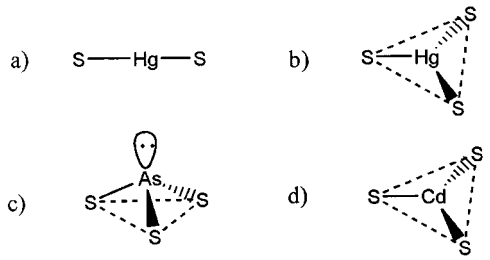

Figure 8. Four metal structure types that have been prepared using the TRI peptide series. (a) Linear Hg(II) as found at low pH in $Hg^{II}(TRI\ L12C)_2$; (b) trigonal planar Hg(II) as found at high pH with $Hg^{II}(TRI\ L16C)_3^-$; (c) trigonal pyramidal As(III) as found at high and low pH in $As^{III}(TRI\ L12C)_3$; (d) trigonal planar Cd(II) as found at high pH with $Cd^{II}(TRI\ L16C)_3^-$.

with chloride ions, TRI L16C forms a thermodynamically more stable bundle with Cd(II) than does TRI L12C. Similarly, ^{113}Cd NMR in the presence of 2 M KCl had slight effects on the chemical shift of either compound, with 7 and 3 ppm upfield shifts for $Cd^{II}(TRIL16C)_3^-$ and $Cd^{II}(TRI\ L12C)_3^-$, respectively. This small shift could be due to problems with the use of an external standard in the NMR experiment that has a very different ionic strength compared to that of the sample. The two complexes, though, shift by a different amount, and that correlates well with all the previous results. The slight $Cd^{II}(TRI\ L12C)_3^-$ chemical shift is consistent with Cd(II) being extracted from the complex by Cl^-, while in the case of $Cd^{II}(TRI\ L16C)_3^-$ there may be an interaction prior to extraction.

This instability of the Cd(II) aggregates in the presence of high chloride concentrations is particularly important when assessing aggregate stability using standard protocols. Strong metal complexes such as $Hg(TRI\ L16C)_3^-$ or $Hg(TRI\ L16C)_2$[38] are unaffected by the high chloride concentrations required for these titrations, and, therefore, meaningful denaturation isotherms can be obtained. In contrast, the chloride is not a spectator ion if Cd(II) is the bound metal. This observation suggests that all investigators examining metal binding to designed peptides should independently assess the impact of chloride on the metal stability prior to obtaining guanidinium denaturation isotherms. Thus, we have achieved our goal of preparing an aqueous soluble and stable peptide aggregate that can enforce a lower coordination onto a bound metal.

The three metals that were used in this study have very distinct geometrical preferences. They all have been observed in a trigonal environment, but only for As(III) is this the preferred coordination number. For Cd(II) and Hg(II), the only examples of such a geometry are with bulky ligands in nonaqueous solutions. In the case of Hg(II) the preferred geometry is linear, while for Cd(II) tetrahedral and octahedral structures prevail. For these metals, both TRI L12C and TRI L16C can either increase the coordination number (e.g., Hg(II)) or decrease the coordination number (e.g., Cd(II)). The apopeptides, on the other hand, can be found, depending on pH, as either parallel two- or three-helical bundles resulting in a linear or trigonal sulfur-binding site. As(III) can be used to enforce a three-stranded α-helical bundle at all pH values for either peptide. At 2:1 peptide-to-metal ratios, Hg(II) will restrict the aggregate solely to the two-stranded α-helical bundle (coiled coil). Thus, the peptide aggregation state can be forced to either increase or decrease the number of α-helices from its preferred apopeptide by judicious choice of metal. Figure 8 summarizes the coordination geometries that can be observed in this peptide class.

Using the metalloregulatory protein MerR, we have previously shown that the TRI peptide family can be used to understand the binding of heavy metals to proteins. Our reevaluation of the extinction coefficients and the bond lengths for Hg(II) binding to TRI L16C demonstrates that the similarity between the two proteins is even more striking than originally suggested. Having garnered spectroscopic data for Cd(II) complexation by TRI L12C and TRI L16C, we can now evaluate cadmium binding metalloregulators. One example is the *Staphylococcus aureus* pI258 CadC protein, which negatively regulates transcription of the Cad operon.[74] Busenlehner et al. have shown that Cd(II) binds to CadC with a 1:1 stoichiometry and a K_d for Cd(II) of 4.3×10^{12} M^{-1}. The Cd^{II}CadC minus apoCadC difference spectrum has a maximum at approximately 240 nm with an extinction coefficient of 25 000 M^{-1} cm^{-1}. These values are, within experimental error, identical to the spectral parameters for $Cd^{II}(TRI\ L12C)_3^-$ and $Cd^{II}(TRI\ L16C)_3^-$ at pH 8.5. Furthermore, the ^{113}Cd NMR of Cd^{II}CadC shows a single resonance at 622 ppm, a value that is strikingly similar to the 625 ppm chemical shift for $Cd^{II}(TRI\ L16C)_3^-$. The EXAFS-derived bond lengths for Cd^{II}CadC (2.53 Å) are a only bit longer than the 2.49 Å observed for $Cd^{II}(TRI\ L12C)_3^-$ or $Cd^{II}(TRI\ L16C)_3^-$. Because of the paucity of good model complexes for Cd(II) in trigonal S_3 environments, the authors could not discern the different coordination modes between S_3O, distorted S_3, or an unusual S_4 coordination structure. Our data would support a Cd(II) geometry in Cd^{II}CadC that is more akin to a distorted S_3 structure with a weak fourth ligand such as water or a sulfidryl.

Conclusions

In summary, we have shown that the TRI peptide family can adopt a variety of aggregation states depending on the pH and metal composition. In cases such as Hg(II), higher coordination numbers can be achieved in aqueous solution at submillimolar concentrations of metal and ligand. The ease of forming trigonal thiolato mercury(II) is dependent on the substitution pattern of the peptide with an *a* position substitution disfavored by approximately 1−2 kcal/mol with respect to substitution at the *d* position. In the case of Cd(II), lower coordination can be achieved. The best description for the coordination environment of the Cd(II) in these complexes (based on ^{113}Cd NMR, CD, EXAFS, and perturbed angular correlation spectroscopy) is a

(74) Busenlehner, L. S.; Cosper, N. J.; Scott, R. A.; Rosen, B. P.; Wong, M. D.; Giedroc, D. P. *Biochemistry* **2001**, *40*, 4426−4436.
(75) See Supporting Information.
(76) Christou, G.; Folting, K.; Huffman, J. C. *Polyhedron* **1984**, *3*, 1247.
(77) Alsina, T.; Clegg, W.; Fraser, K. A.; Sola, J. *J. Chem. Soc., Dalton Trans.* **1992**, 1393.
(78) See Supporting Information.
(79) Hemmingsen, L.; Bauer, R.; Bjerrum, M. J.; Adolph, H. W.; Zeppezauer, M.; CedergrenZeppezauer, E. *Eur. J. Biochem.* **1996**, *241*, 546−551.
(80) Hemmingsen, L.; Bauer, R.; Bjerrum, M. J.; Zeppezauer, M.; Adolph, H. W.; Formicka, G.; Cedergrenzeppezauer, E. *Biochemistry* **1995**, *34*, 7145−7153.
(81) Bauer, R.; Danielsen, E.; Hemmingsen, L.; Sorensen, M. V.; Ulstrup, J.; Friis, E. P.; Auld, D. S.; Bjerrum, M. J. *Biochemistry* **1997**, *36*, 11514−11524.
(82) Bauer, R.; Christensen, C.; Johansen, J. T.; Bethune, J. L.; Vallee, B. L. *Biochem. Biophys. Res. Commun.* **1979**, *90*, 679−685.
(83) Danielsen, E.; Bauer, R. *Hyperfine Interact.* **1990**, *62*, 311−324.
(84) Bauer, R.; Demeter, I.; Hasemann, V.; Johansen, J. T. *Biochem. Biophys. Res. Commun.* **1980**, *94*, 1296−1302.
(85) Bauer, R.; Danielsen, E.; Hemmingsen, L.; Bjerrum, M. J.; Hansson, O.; Singh, K. *J. Am. Chem. Soc.* **1997**, *119*, 157−162.

trigonal planar S_3 structure with, in some cases, a small component of distorted trigonal planar geometry. On the basis of the remarkably similar spectral parameters between Cd^{II}(TRI L16C)$_3^-$ and Cd^{II}CadC, we propose that this metalloregulatory protein is best described as having a dominant S_3 coordination sphere which is either trigonal planar or slightly distorted from this geometry. Future studies using the TRI peptides with other heavy metals such as Pb(II) may help to unravel further the coordination geometry of heavy metals with transcriptional regulatory proteins.

Acknowledgment. The authors thank Prof. Gregg Dieckmann and Prof. William DeGrado for early collaboration on this project and for useful discussions on these systems. We thank Prof. T. V. O'Halloran for commenting on this manuscript prior to submission. B.T.F. thanks the National Institutes of Health for NRSA Fellowship Grant 1F32 ES05888-01.

Supporting Information Available: UV−vis titration of TRI L12C into a solution of Cd(II) at pH 8.5; UV−vis titration of TRI L12C into a solution of Cd(II) at pH 9.4 in 20 mM MES buffer; normalized Cd(II) XANES spectra; references for the CdS_3, CdS_4, HgS_2, and HgS_3 models used in the EXAFS study (PDF). This material is available free of charge via the Internet at http://pubs.acs.org.

JA017520U